scientific reports

Check for updates

OPEN

PknB and STP as potential targets of luteolin in combating *Trueperella pyogenes* infections

Yueting Guo, Hongyu Su, Lihui Yu, Yingyu Wang, Chunlian Tian, Dexian Zhang, Yuru Guo✉ & Mingchun Liu✉

Trueperella pyogenes **(*T. pyogenes*) is a significant opportunistic pathogen that causes suppurative infection in many animals, as well as humans. Considering the strong drug resistance of *T. pyogenes*, the development of novel antibacterial drugs and drug targets to combat infections is necessary. Serine/threonine protein kinases (STKs) and serine/threonine phosphatases (STPs) play pivotal roles in the physiological processes, pathogenesis, and resistance of several important bacterial pathogens, indicating their potential as antimicrobial drug targets. In this study, we aimed to investigate the effects of luteolin, a natural flavonoid, on serine/threonine protein kinase B (PknB) and serine/threonine phosphatase (STP). The results revealed that after *T. pyogenes* was treated with 1/2 MIC (39 μg/mL) luteolin for 36 h, the transcription and translation levels of the *pknB* and *stp* genes decreased significantly. Molecular docking revealed that hydrophobic forces were predominant in the interaction between luteolin and PknB, whereas hydrogen bonding was predominant in the interaction between luteolin and STP. The results of the molecular interaction assay revealed that the K_D value of luteolin with PknB and STP were 3.125×10^{-4} M and 1.128×10^{-5} M, respectively. Additionally, luteolin could inhibit the activities of PknB and STP. Our study demonstrated that luteolin can inhibit PknB and STP at multiple levels, and it is expected to be used as a PknB/STP inhibitor to develop new drugs against drug-resistant bacterial infections.**

Keywords *Trueperella pyogenes*, Luteolin, PknB, STP, Drug target, Inhibitor

Trueperella pyogenes (*T. pyogenes*) is an opportunistic, gram-positive bacterium that causes various infections such as mastitis, pneumonia, liver abscess, metritis, endocarditis, and osteoarthritis. These infections not only cause significant economic losses in the animal husbandry industry but also pose a serious threat to human health and safety[1,2]. Aminoglycosides, β-lactams, tetracyclines, macrolides, and fluoroquinolones are commonly used to treat *T. pyogenes* infections; however, their use may contribute to the emergence of antimicrobial resistance. The development of antimicrobial resistance in *T. pyogenes* has become a formidable obstacle inhibiting its clinical management[3–6]. Consequently, the exploration of novel drug targets and drugs that can effectively combat *T. pyogenes* infections is crucial.

Bacteria can survive under a variety of environmental stimuli. Adaptability is largely attributed to the presence of diverse protein kinases, which enable bacteria to sense and respond to external signals[7]. Signal transduction via reversible phosphorylation is important for environmental adaptation and virulence in pathogenic bacteria[8]. A two-component system, which is composed of histidine kinases (HKs) and response regulators (RRs), is involved in multiple bacterial behaviors by regulating quorum sensing, bacterial pathogenicity, and antimicrobial resistance[9–12]. However, recent studies have revealed that eukaryotic-like serine/threonine kinases (eSTKs) and eukaryotic-like serine/threonine phosphatases (eSTPs) are widely distributed in bacteria and are important regulators of several important bacterial pathogens, including *Mycobacterium tuberculosis*, *Streptococcus pneumoniae*, *Listeria monocytogenes*, and *Streptococcus suis*[13–17]. In *Streptococcus pyogenes*, both STK and STP participate in cell division, adhesion to, and invasion of, epithelial cells, and virulence. *Mycobacterium tuberculosis* involves eleven Ser/Thr kinases, two of which, PknA and PknB, regulate essential physiologies and antimicrobial susceptibility of *Mycobacterium tuberculosis*[18]. Based on their critical physiological roles, STK and STP have the potential to be developed as drug targets. In our previous study, we reported that serine/threonine protein kinase

Key Laboratory of Livestock Infectious Diseases, Ministry of Education, and Key Laboratory of Ruminant Infectious Disease Prevention and Control (East), Ministry of Agriculture and Rural Affairs, College of Animal Science and Veterinary Medicine, Shenyang Agricultural University, 120 Dongling Road, Shenyang 110866, China. ✉email: yuruguo0821@syau.edu.cn; liumingchun@syau.edu.cn

B (PknB) and serine/threonine phosphatase (STP), which have potential as drug targets to combat *T. pyogenes* infections, are present in *T. pyogenes*.

Natural plant products are valuable resources for screening new antibacterial drugs. Luteolin is a natural secondary flavonoid and is widely distributed in vegetables and medicinal plants such as broccoli, honeysuckle, and chrysanthemum. Luteolin exhibits antioxidant, anti-inflammatory, anti-tumor, and antimicrobial effects[19,20]. Our previous findings indicated that luteolin could inhibit the growth of *T. pyogenes* by affecting different cellular components, such as the cell wall, cell membrane, nucleic acid, and proteins[21]. Additionally, luteolin could increase the susceptibility of *T. pyogenes* to aminoglycosides and macrolides by inhibiting MATE and the MsrA efflux pump[22,23]. Our recent studies demonstrated that luteolin can also inhibit the biofilm formation of *T. pyogenes*. Luteolin decreased the expression of biofilm-related genes such as *luxS*, *rbsB*, and *lsrB*[24]. These findings suggest that luteolin has great potential as an effective anti-biofilm agent against *T. pyogenes*.

In recent years, many natural compounds, particularly protein kinase inhibitors, have been identified as potential drug candidates. These compounds serve as promising starting points for the development of new substances with therapeutic properties[25]. For example, a study demonstrated that matrine acts as a novel inhibitor of protein kinase C phosphorylated kinase, thereby inhibiting hepatitis B virus replication through the regulation of mitogen-activated protein kinase signalling[26]. Another study revealed that luteolin inhibited the autophosphorylation activity of the typical histidine kinase (HK853) in *Thermotoga maritime* by occupying the binding pocket of adenosine diphosphate (ADP) through hydrogen bonding and π–π superposition[27]. Researches have indicated that luteolin and several other flavones possess the ability to inhibit kinase enzymes[28–31]. For instance, casein kinase 2 (CK2) is a serine/threonine protein kinase related to gene expression, protein synthesis degradation in eukaryotic cells, and luteolin can interact with CK2 and inhibit its activity[32].

However, there are no pertinent reports documenting the effects of flavonoids on the serine/threonine kinase and phosphatase activities of *T. pyogenes*. The primary objective of this study was to determine the potential of luteolin as an inhibitor of PknB and STP in *T. pyogenes*-induced infections.

Materials and methods

Animals

Female New Zealand white rabbits (3 mouths of age) were purchased from Kang da Biological Technology Co., Ltd. (Qingdao, China, Permit No.: SCXK (Lu) 2016-0002) and reared under pathogen-free conditions for immunization. All the experiments were performed according to the Guidelines of Animal Experiments of Shenyang Agricultural University, and efforts were made to minimize suffering. The protocol was approved by the Ethics Committee of Shenyang Agricultural University (SYXK(Liao)2021-0010, Shenyang, China). The study was carried out in accordance with the ARRIVE guidelines.

Strains, media and growth conditions

The *T. pyogenes* strain ATCC19411 was purchased from the American Type Culture Collection (Manassas, VA, USA). Seventeen *T. pyogenes* isolates (T001-T017) were obtained from dairy cows and preserved in our laboratory. The *T. pyogenes* isolates were cultured on Mueller–Hinton agar (MH(A), AOBOX, Beijing, China) supplemented with 5% sterile defibrinated sheep blood (Solarbio, Beijing, China) for 48 h at 37 °C in 5% CO_2. Three to five colonies were subsequently inoculated in brain heart infusion (BHI) medium (Solarbio, Beijing, China) supplemented with 8% (v/v) foetal bovine serum (FBS; Gibco, Grand Island, United States) for 24 h at 37 °C with shaking at 180 rpm. Luteolin (purity ≥ 98%) was purchased from Shanghai Pureone Biotechnology Co., Ltd. (Shanghai, China) and dissolved in 1% dimethyl sulfoxide (DMSO, Sigma-Aldrich, Shanghai, China) as a stock solution. It was stored at − 20 °C before use.

Screening of the *pknB* and *stp* genes

The *pknB*- and *stp*-positive strains were identified via PCR. The primers for *pknB* and *stp* are listed in Table 1. Each PCR reaction included 5 µL of PrimeSTAR Max (Premix) (2x; TaKaRa, Dalian, China), 0.2 µL of each primer, 0.5 µL of template DNA and nuclease-free water in a total volume of 10 µL. The PCR conditions were as follows: 35 cycles of denaturation at 98 °C for 10 s, annealing at 61 °C for 5 s, and extension at 72 °C for 10 s. After PCR amplification, the products were extracted using 1% agarose (Sigma, Shanghai, China) gel electrophoresis. Gel imaging analysis was performed via the Azure Biosystems C300 system (United States), and photographs were taken. The PCR products were sent to Sangon Biotech Company (Shanghai, China) for sequencing. The obtained gene sequences were then compared with the *pknB* and *stp* gene sequences recorded in NCBI for BLAST analysis.

Gene	Sequence (5′-3′)	Product size (bp)	Temperature (°C)
pknB	forward: ATGGCGTCGGTGAGCGAC	998	56.9
	reverse: TCAGTGTCCAATCTGTGCGAGA		
stp	forward: CGGGATCCATGGCTGACGTACCCCGAA	732	61
	reverse: CCCAAGCTTTCGATTGTGTTTGTTCTCTTCAACCG		

Table 1. Primer sequences for PCR used in this study.

Gene	Sequence (5′-3′)	Product size (bp)	Temperature (°C)
pknB	forward: TCGACTTCTCACCACTGAACAC	188	56.9
	reverse: CTTTCATCAGTGCAAGCGTGA		
stp	forward: TCGTCGTCGGCATCCTGTCC	112	61
	reverse: TTGTCTGCGTCATTGTGGCTGAG		
gapdh	forward: CGGCGAAGAACGAGGACATCAC	153	63.5
	reverse: GTCGGCAGTGTAGGCGTGAAC		

Table 2. Primer sequences for qPCR used in this study.

Gene	Sequence (5′-3′)	Product size (bp)	Temperature (°C)	Restriction site
pknB	forward: CGGGATCCATGG CTGACGTACCCCGAA	998	56.9	*Bam*H I
	reverse: TAAAGCGGCCG CTTACGGCCGAACAGATGGCGTA			*Hin*d III
stp	forward: CGGGATCCATGG CTGACGTACCCCGAA	732	61	*Bam*H I
	reverse: CCCAAGCTTTCGATTG TGTTTGTTCTCTTCAACCG			*Hin*d III

Table 3. Primer sequences used in the expression of the His-PKNB and His-STP fusion proteins.

Analysis of the expression of *pknB* and *stp* using quantitative real-time PCR

Quantitative real-time PCR (qRT-PCR) was conducted to detect the expression levels of the *pknB* and *stp* genes after luteolin treatment of *T. pyogenes* for 36 h. In this study, *gapdh* was used for normalization as endogenous reference gene and the relative expression levels of *pknB* and *stp* genes were calculated via the $2^{-\Delta\Delta Ct}$ method. The treatment protocol for the *T. pyogenes* samples was the same as previously described[23]. Briefly, *T. pyogenes* cultured to the logarithmic phase was diluted to 1×10^6 CFU/mL and mixed with 1/2 MIC luteolin (final concentration, 39 μg/mL); the bacterial suspensions were cultured at 37 °C for 36 h. The bacterial suspensions treated with the same final concentration of DMSO (v/v, 0.01%) were employed as a solvent control. Total RNA from *T. pyogenes* was extracted via TRIzol Reagent (Ambion, Carlsbad, USA) following the manufacturer's instructions. cDNA synthesis was subsequently carried out via a PrimeScript RT Reagent Kit with gDNA Eraser (TaKaRa, Dalian, China). The transcription levels of the *pknB* and *stp* genes were detected via the TB Green Premix Ex TaqTM II Kit (TaKaRa, Dalian, China) on the Applied Biosystems QuantStudio 3 Real-Time PCR System (Thermo Fisher, USA). The conditions for qRT-PCR were as follows: predenaturation at 95 °C for 30 s; then, 40 cycles of 95 °C for 5 s, 60 °C for 30 s and 72 °C for 30 s. The primer sequences are listed in Table 2. The threshold cycle (Ct) values were obtained from the qRT-PCR reaction. Compared to the *gapdh* gene (internal control), the relative expression of the target gene was calculated using the $2^{-\Delta\Delta Ct}$ method ($\Delta Ct = Ct$ target gene $- Ct$ internal control, and $\Delta\Delta Ct = \Delta Ct$ test sample $- \Delta Ct$ control sample in each sample), as previously described[33]. The data are presented as the means ± standard deviations (SDs) derived from three independent experiments.

Protein expression and purification

The primers used for amplification of the complete gene sequences of *pknB* and *stp* carrying restriction sites are listed in Table 3. The PCR products of *pknB* and *stp* carrying *Hin*d III and *Bam*H I restriction sites were inserted into the digested pET-28a vector to generate the recombinant plasmids pET-28a-*pknB* and pET-28a-*stp*. These plasmids were transformed into BL21(DE3) *E. coli* competent cells (TransGen Biotech) for protein expression. When the cell density reached an OD_{600} of approximately 0.6, the cells were induced to express His-PknB and His-STP fusion proteins by adding 1 mM isopropyl-β-D-thiogalactopyranoside (IPTG) (Sigma, USA) and incubating at 22 °C for 16 h. The fusion proteins His-PknB and His-STP were purified via Ni-NTA columns (TaKaRa, Dalian, China) following the manufacturer's recommendations. The purified proteins were then identified by Western blot analysis using a corresponding alkaline phosphatase-conjugated anti-polyhistidine monoclonal antibody (BBI Life Science, Shanghai, China).

Preparation of polyclonal antibodies against His-PknB and His-STP proteins

The purified His-PknB and His-STP fusion proteins were used as antigens to prepare polyclonal antibodies. Adult female New Zealand white rabbits were used to generate antibodies. Approximately 0.4 mg of purified His-PknB was emulsified with an equal volume of Freund's Complete Adjuvant (Sigma, Shanghai, China) and injected subcutaneously at multiple sites along the backs of New Zealand white rabbits. Following an initial immunization period of 15 days, the protein was mixed with Freund's Incomplete Adjuvant (Sigma, Shanghai, China) for booster immunizations on the 7th, 14th, and 21st days. One week after the final immunization, rabbits were anesthetized with isoflurane and their sera were separated. A similar methodology was applied to generate polyclonal antibodies against recombinant His-STP. Antibody titers were determined by indirect ELISA, utilizing the respective antigen as the coating antigen and the pre-immunization serum of each rabbit as the negative control.

The pGEX4T-1 vectors were used to express the fusion proteins GST-PknB and GST-STP, which carry a glutathione S-transferase (GST) tag. The fusion proteins GST-PknB and GST-STP were purified via glutathione sepharose affinity. GST-PknB and GST-STP were used as antigens to determine the titers of anti-PknB and anti-STP polyclonal antibodies via ELISA. Once the titer reached 1:16,000, the serum of the rabbits was collected and stored at − 80 °C.

Analysis of the expression levels of PknB and STP via Western blotting

Western blotting was used to detect the expression levels of PknB and STP of *T. pyogenes* after luteolin treatment for 36 h. The method of treating *T. pyogenes* with luteolin is same as decreased in "Analysis of the expression of *pknB* and *stp* using quantitative real-time PCR". Total protein extraction from *T. pyogenes* and luteolin treatment were conducted according to the protocol reported by Guo et al[23]. SDS-PAGE of protein samples was performed, and then the protein samples were transferred to polyvinylidene difluoride (PVDF) membranes (Millipore, Shanghai, China). Anti-His-PknB or anti-His-STP polyclonal antibodies were used as the primary antibodies, and horseradish peroxidase (HRP)-conjugated goat anti-rabbit immunoglobulin G (IgG) was used as the secondary antibody. Glyceraldehyde 3-phosphate dehydrogenase (GAPDH) was used as a reference protein. The membranes were visualized via the Azure C300 imaging system (Azure, Dublin, USA). The Western blot analyses were performed in at least three replicates for each protein, and the intensity of the protein bands was quantified via ImageJ software (http: //developer.imagej.net/development).

Molecular docking of luteolin with the PknB and STP proteins

The three-dimensional (3D) structures of the PknB and STP proteins were predicted via the homology modelling technique. The protein sequences were uploaded to https://swissmodel.expasy.org/, an online prediction tool, and then the homologous proteins with a high degree of sequence homology were identified as templates. The 3D structures of PknB and STP were built according to the templates, and the PDB files were stored for subsequent molecular docking. The 3D structure of luteolin was sketched via ChemDraw Ultra 7.0, energy-minimized via Chem3D Ultra 7.0, and saved as a PDB file for ligands. CB-Dock2 (https://cadd.labshare.cn/cb-dock2/php/index.php) is a molecular docking tool that utilizes AutoDock Vina analysis[34,35] to automatically identify and analyze the binding sites of ligands and receptors. The molecular docking between luteolin and PknB/STP was predicted via CB-Dock2, and the details of the ligand-receptor interactions were analyzed. The three-dimensional (3D) interaction mode was generated by the Protein–Ligand Interaction Profiler (PLIP) and PyMol v2.6 software[36,37], while BIOVIA Discovery Studio (DS) Visualizer 2021 software was employed to create the interaction two-dimensional (2D) diagrams.

Detection of the interaction between luteolin and PknB/STP

Surface Plasmon Resonance (SPR) technology has been proven to be a significant approach for target-based drug discovery and development in the modern era[38]. The interaction between luteolin and PknB/STP was determined via surface plasmon resonance (SPR) technology on a Biacore T200 system (GE Healthcare, Sweden) equipped with an NTA sensor chip (GE Healthcare). The proteins were diluted with 1 × PBS-P buffer to achieve a final concentration of 30 μg/mL, resulting in a coupling level of approximately 3000 RU. Luteolin was diluted to a series of concentrations (0.3125, 0.625, 1.25, 2.5, 5, and 10 μmol/L) in 1 × PBS-P buffer and flowed through the chip surface with PknB/STP protein coupling. Finally, the data obtained were analysed via Biacore T200 evaluation software, and the association constant (K_a), dissociation constant (K_d) and the equilibrium dissociation constant (K_D) were determined.

Determination of luteolin's effects on PknB and STP activities

PknB phosphorylates itself by hydrolyzing ATP. Therefore, the kinase activity can be determined by measuring the consumption of ATP. The kinase activity detection assay was performed in 50 μL of kinase reaction buffer (Tris-HCl 50 mM, DTT 1 mM, pH 7.8) containing 10 mM $MgCl_2$, 20 μM ATP, 2 μg PknB, and different concentrations of luteolin or DMSO. The reaction mixtures were incubated at 25 °C for 30 min. Subsequently, 50 μL of Kinase-Lumi™ Reagent (Beyotime, Shanghai, China) was added to each well. After a 10-min incubation, relative luminescence units (RLU) were measured using a multimode plate reader (VICTOR Nivo). Inhibition percentage was calculated as $(RLU_X - RLU_P)/(RLU_N - RLU_P) \times 100\%$, where RLU_X is the RLU value for a test treated with compound X, and RLU_P and RLU_N are the RLU values for the reaction mixture without the treatment of compound and the reaction mixture lacking PknB, respectively.

Phosphatase activity was detected as previously described[43]. Briefly, reactions were performed in 100 μL mixture (containing 50 μg/mL STP in p-nitrophenyl phosphate (pNPP) buffer 25 mM Tris-HCl, pH 7.5, 4 mM $MnCl_2$, 0.1 mM EDTA, 0.02% β-mercaptoethanol) and the various concentrations of luteolin (5, 10, 20, 40, and 80 μg/mL). The reaction mixtures were incubated at 37 °C for 30 min to allow inhibitor-enzyme interaction and initiated by adding pNPP to a final concentration of 1 mM and incubated at 37 °C for 30 min. Finally, 50 μL 1 M NaOH was added to quench the reaction, and the absorbance was measured at 405 nm. The absorbance was calculated as a percentage of the phosphatase activity and plotted as a function of inhibitor concentration to determine the half-maximal inhibitory concentration (IC_{50}) of luteolin for STP. The data that were displayed on a log scale were log-transformed and non-linear regression was conducted using GraphPad Prism 8.0 with the variable slope normalized model for enzyme inhibition to ascertain IC_{50}. The experiments were carried out three times independently under the same conditions.

Statistical analysis

The Western blot and qRT-PCR results are presented as the means ± standard deviations (SDs) of three separate experiments. Statistical analysis and independent Student's tests were performed via GraphPad Prism 8.0 and SPSS Statistics V17.0. Statistical significance was defined as $^{*}P < 0.05$ and $^{**}P < 0.01$.

Results

Effects of luteolin on the transcription levels of *pknB* and *stp*

The *pknB* and *stp* genes were detected across all the *T. pyogenes* isolates. To investigate the effect of luteolin on the transcription levels of *pknB* and *stp* genes, qRT-PCR analysis was conducted after luteolin treatment on *T. pyogenes*. As shown in Fig. 1, there were significant reductions in the expression of *pknB* and *stp* genes after luteolin treatment. Specifically, compared with that in the control group, the expression of *pknB* gene decreased to 8.0–72.7%, while the expression of *stp* gene decreased to 4.3–71.6%. These results indicated that luteolin could reduce the transcription levels of *pknB* and *stp* genes in *T. pyogenes*.

Effects of luteolin on the translation levels of PknB and STP

Polyclonal antibodies against His-PknB and His-STP were generated by immunizing New Zealand white rabbits. The purification and identification results of His-PknB and His-STP are presented in Fig. 2A and D, which indicate that His-PknB and His-STP were successfully obtained. Similarly, GST-PknB and GST-STP were successfully obtained, as shown in Fig. 2B and E. The ELISA results indicated that the titers of the anti-His-PknB and anti-His-STP polyclonal antibodies reached 1:2,048,000, providing evidence for the ability of rabbit antiserum to recognize the PknB and STP proteins (Fig. 2C and F). Subsequently, anti-His-PknB and anti-His-STP polyclonal antibodies were used in Western blot assays to analyse the protein expression of PknB and STP in *T. pyogenes*. Three separate Western blot assays were performed, among which one representative Western blot is shown in Fig. 3A and B. As depicted in Fig. 3C, compared with that in the control group, the relative expression level of PknB in 18 T. *pyogenes* strains decreased to 26.7–73.1% after luteolin treatment. Similarly, luteolin also significantly reduced the protein expression level of STP (decreased to 25.9–72.6%) (Fig. 3D).

Molecular docking of luteolin and PknB/STP

To explore the interaction between luteolin and the PknB/STP proteins, molecular docking analysis was performed via CB-Dock 2. The theoretical three-dimensional binding mode of luteolin and PknB is illustrated in Fig. 4A and B. The simulation results revealed that luteolin was able to interact with the primary amino acid residues on the active site of PknB. The binding energy of luteolin and PknB was -8.9 kcal/mol, which indicated good binding ability. The 3D and 2D interaction plot of the luteolin-PknB complex is presented in Fig. 4C and D. We found that luteolin was positioned at the hydrophobic pocket, surrounded by the residues ALA41, LEU20, MET148, MET95, MET158 and VAL28, forming a stable hydrophobic binding. Among these amino acid residues, most of them belong to protein kinase domain. As illustrated in Fig. 4E and F, the theoretical three-dimensional binding mode of luteolin and STP is presented. The binding energy between luteolin and STP was − 7.4 kcal/mol. The binding interactions primarily involved hydrogen bonding and van der Waals forces, with the key interacting residues being ASP192, GLN137, ALA150, VAL136, ARG156, ARG177 and HIS151 (Fig. 4G and H). Among these amino residues, all belong to the PPM-type phosphatase domain. Therefore, it is predicted that luteolin may inhibit the activity of protein kinases and phosphatases by binding to the key amino acid residues of the PknB and STP proteins. These results indicate that luteolin exhibits a strong binding affinity for the PknB/STP proteins.

Affinity of luteolin with PknB/STP

The affinity between luteolin and PknB or STP was determined via the Biacore T200 system to verify the possibility of interaction of luteolin with PknB and STP. The sensor diagram and fitting curve are shown in Fig. 5. The binding and dissociation curves revealed the rapid binding and slow dissociation patterns of luteolin and PknB/STP. Through analysis of the fitting parameters, it was determined that the K_D value of the luteolin and

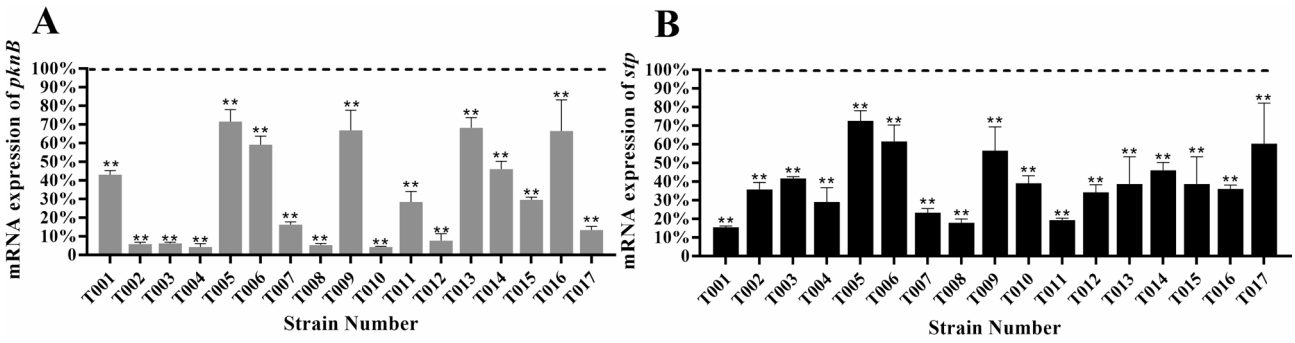

Fig. 1. The mRNA expression level of *pknB* and *stp* genes in 17 T. *pyogenes* after luteolin treatment. (**A**) The mRNA expression of *pknB*, (**B**) the mRNA expression of *stp. T. pyogenes* treated with luteolin at 1/2 MIC. Data were presented as means ± SD. (*compared with the solvent control, $^{*}P < 0.05$, $^{**}P < 0.01$).

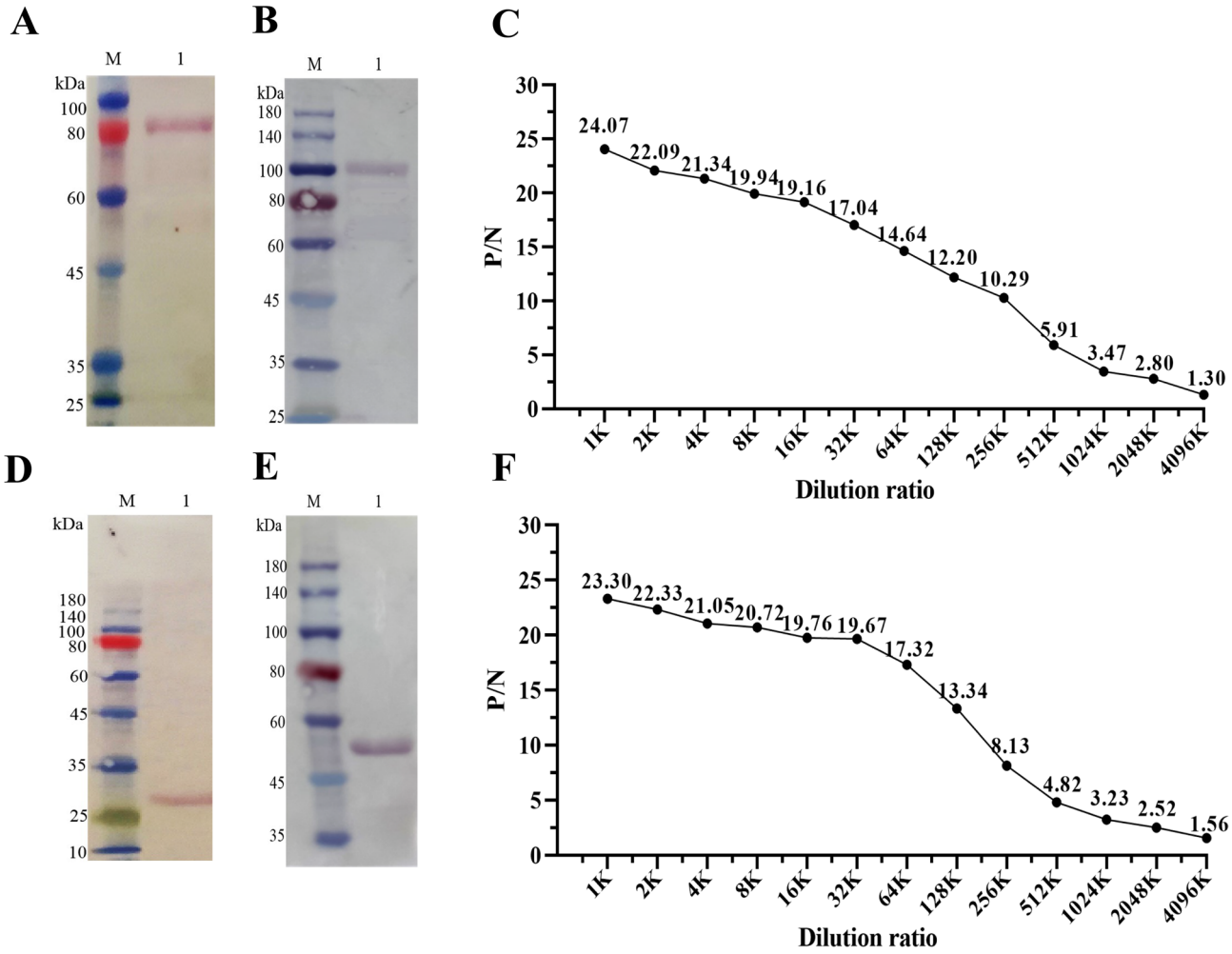

Fig. 2. Preparation of the anti-PknB and anti-STP polyclonal antibodies. (**A**, **D**) Western blot analysis of purified His- PknB and His-STP fusion proteins using an anti-His monoclonal antibody. (**B**, **E**) Western blot analysis of purified GST- PknB and GST-STP fusion proteins using an anti-GST monoclonal antibody. (**C**, **F**) Detection of serum titer of anti-His- PknB and His-STP proteins by ELISA.

PknB/STP proteins were 3.125×10^{-4} M and 1.128×10^{-5} M, respectively. These findings indicate that luteolin can stably bind to PknB and STP.

Effects of luteolin on PknB and STP activities

To further assess the effect of luteolin on the activity of PknB and STP, the kinase and phosphatase activity detection assays were conducted to determine the IC_{50} of luteolin. It was shown in Fig. 6A that the IC_{50} of luteolin against PknB was 63.28 μg/mL. The data further verified the inhibitory effect of luteolin on PknB. Additionally, luteolin inhibited the activity of STP in a dose-dependent manner. The IC_{50} of luteolin on STP was 47.72 μg/mL (Fig. 6B).

Discussion

Infections caused by *T. pyogenes* pose a serious threat to animal husbandry, endangered species protection, and human health. Additionally, the antimicrobial resistance of *T. pyogenes* is critical, and novel anti-infection strategies to combat *T. pyogenes* are urgently needed. STKs and STPs play important roles in cell division, metabolism, virulence, resistance, and pathogenesis in many important bacterial pathogens[8].

The significant functions of reversible protein phosphorylation orchestrated by bacterial kinases and phosphatases have been duly acknowledged in recent decades, with various bacterial protein kinases being proposed as viable candidates for novel antibiotic targets[39]. Several inhibitors that target STK, including staurosporine, K252a, AT9283, and APY29, have recently been discovered. These inhibitors have a significant inhibitory effect on the growth of *Streptococcus. suis* in minimal medium[40]. Chen D. and colleagues reported that sclerotiorin inhibited protein kinase G in *Mycobacterium tuberculosis* and impaired the growth of mycobacterial macrophages[41]. Flavanones were identified as potential natural inhibitors of the ATP binding site of PknG in *Mycobacterium tuberculosis* and play crucial roles in regulating bacterial metabolism for survival in host macrophages[42]. Zheng et al. reported that aurintricarboxylic acid (ATA) bound Stp1 directly and inhibited

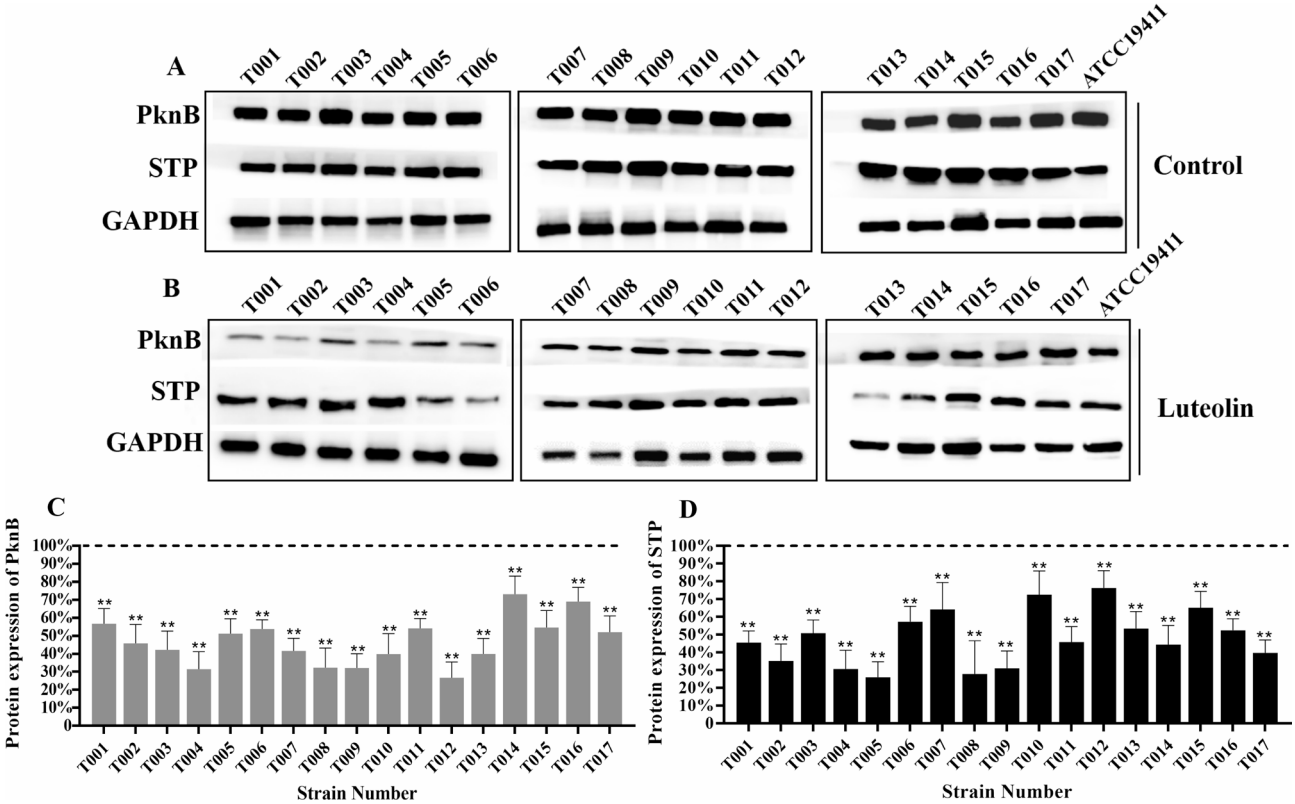

Fig. 3. The effect of luteolin on the expression of PknB and STP in 17 T. *pyogenes*. (**A**, **B**) Western blot results PknB and STP in *T. pyogenes* with different treatment, (**C**) the protein expression of PknB, (**D**) the protein expression of STP. *T. pyogenes* treated with luteolin at 1/2 MIC. Data were presented as means ± SD. (*compared with the solvent control, $^{*}P < 0.05$, $^{**}P < 0.01$).

its activity and that ATA was a potent Stp1 inhibitor against staphylococcal infection[43]. However, inhibitors targeting *T. pyogenes* PknB and STP have not been reported.

Luteolin, a representative natural flavonoid, is widely distributed in nature. Recent studies have verified that luteolin not only has good antibacterial activity but also inhibits the formation of bacterial biofilms and the expression of virulence genes[24,44,45]. Studies have shown that luteolin has anti-quorum-sensing (QS) and anti-biofilm abilities against *Pseudomonas aeruginosa*[46]. This is achieved by downregulating the QS signal molecules OdDHL and BHL, inhibiting the relative expression of QS genes, and competing with OdDHL for binding to the LasR receptor protein[47].

In this study, we found that luteolin significantly inhibited the transcription and translation levels of the *pknB* and *stp* genes. In addition, luteolin can interact with important amino acid residues of the PknB and STP proteins. Furthermore, luteolin significantly inhibited the activity of PknB and STP. It is hypothesized that it may be due to the tight binding between the inhibitor and the active region of the protein that it is able to compete with the substrate, thus reducing the catalytic ability of the active site and leading to a decrease in protein activity. These results indicate the potential of luteolin as a potential inhibitor of PknB and STP to combat the antimicrobial resistance, virulence, and other biological activities of bacteria. However, the specific effect and mechanism of luteolin on *T. pyogenes* through PknB/STP need to be further explored. Our results suggest the feasibility of luteolin as an inhibitor of PknB and STP and provide a theoretical basis for the development of new antibacterial drugs based on natural compounds in the future.

To date, a number of researches have reported the application of SPR in detecting the interaction between drug molecules and target proteins. This technology can accelerate the screening process of new drugs and improve efficiency, significantly saving research and development costs. Early study has reported that luteolin could bind to the N-terminal of ATP/ADP-binding domain of Hsp90. The stability of this interaction was further confirmed by SPR analysis, suggesting that luteolin may act as a potent Hsp90 inhibitor for antitumor strategies[48]. Previous work demonstrated that luteolin bound to the L85 and S155 residues of the CviR protein of *Chromobacterium violaceum*, suggesting that luteolin interacts with the CviR quorum-sensing regulator, influencing the formation of bacterial biofilms and regulating bacterial virulence[49]. In prior studies, we ascertained that luteolin inhibited the activities of MsrA and TatD DNases in *T. pyogenes* by binding with them[23,44].

In this study, the molecular docking results revealed that the PknB and STP proteins had strong affinities with luteolin, and the 3D and 2D structures of combinations of these proteins were presented. The PknB and STP proteins bind to luteolin mainly through hydrophobic forces and hydrogen bonds, respectively. Furthermore, the low free energy between luteolin and PknB/STP demonstrated that the active sites of the PknB and STP proteins

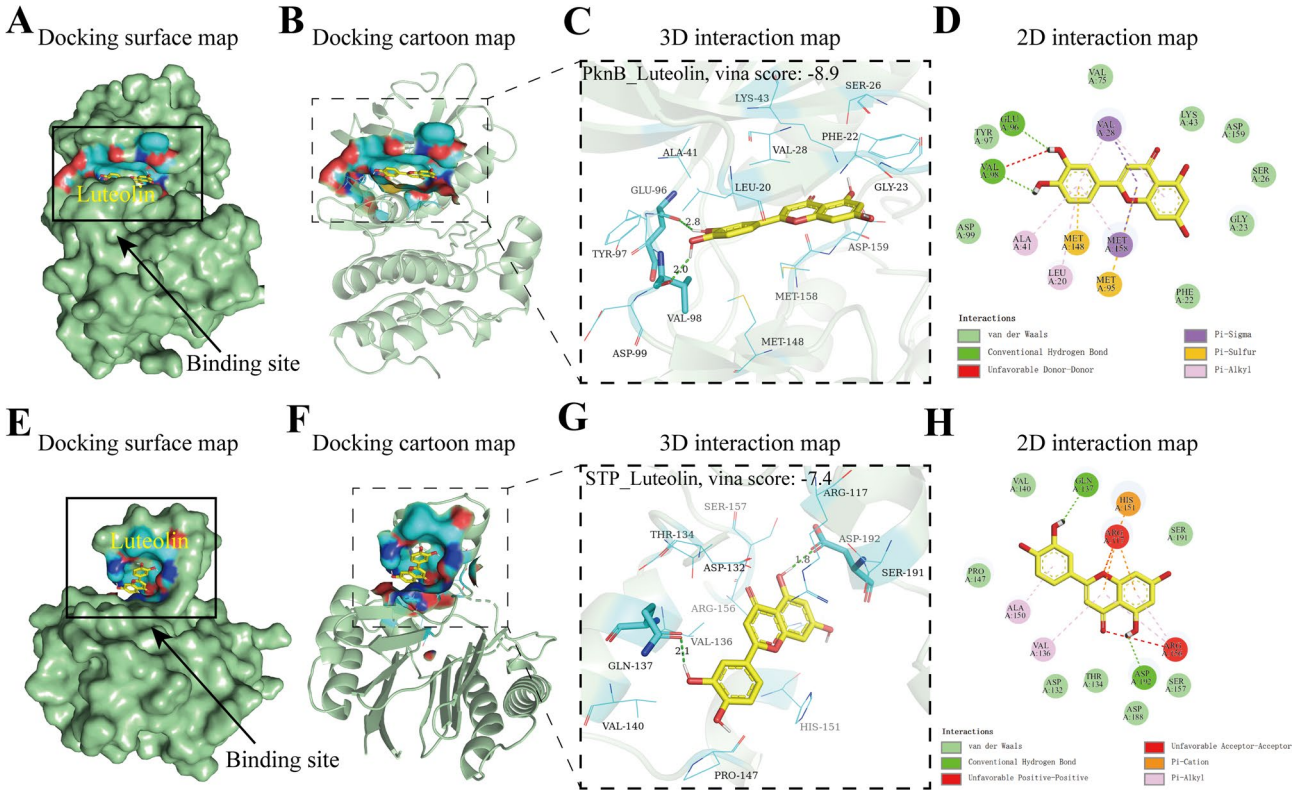

Fig. 4. The molecular docking results of luteolin and the PknB or STP protein. (**A**, **E**) docking surface map of luteolin with PknB and STP, (**B**, **C**, **F**, **G**) show luteolin interacting with the amino acid residues located within the active sites of the PknB and STP pockets in three-dimensional (3D) docking models, (**D**) show the interactions between luteolin and PknB in two-dimensional (2D) docking model, (**H**) show the interactions between luteolin and STP in two-dimensional (2D) docking model.

were well occupied by luteolin and that their binding was highly stable. The affinity fitting results in this study illustrated that luteolin and PknB/STP could form a relatively stable combination. It has been postulated that the PknB and STP proteins are potential targets of luteolin.

These findings provide a theoretical foundation for the use of luteolin as a natural antibacterial agent that targets the PknB/STP proteins. Therefore, further studies are needed to elucidate the effects of luteolin on pathogenicity and antimicrobial resistance though the targeting of PknB or STP in *T. pyogenes*.

There are still some limitations in this study. Due to constraints related to time and resources, only a preliminary exploration was conducted, and a comprehensive investigation into the action mechanism of luteolin on PknB and STP was not performed. For example, the effects of luteolin on the structure of target proteins and downstream signaling pathways remain unknown. Furthermore, the biological functions of PknB and STP in *T. pyogenes* were not examined in this study, leading to ambiguity regarding their roles in the organism. These gaps preclude comprehensive assessment of luteolin's potential as a targeted anti-*T. pyogenes* agent. Future studies will aim to address these gaps through CRISPR-Cas9-mediated gene knockout, multi-omics techniques and X-ray crystallography.

Conclusions

This study aimed to explore the regulatory effects of luteolin on the expression of PknB and STP, as well as the interaction between luteolin and PknB/STP, including their binding sites. These results presented compelling evidence supporting the potential of luteolin as an inhibitor of the PknB and STP proteins of *T. pyogenes*. Our findings demonstrated a significant inhibitory effect of luteolin on the transcription and translation of the *pknB* and *stp* genes. Additionally, luteolin could inhibit the activities of PknB and STP. Furthermore, our results indicated that luteolin could interact with the key amino acid residues of PknB and STP. Luteolin is a promising candidate for the development of novel antibacterial agent to combat *T. pyogenes* infections.

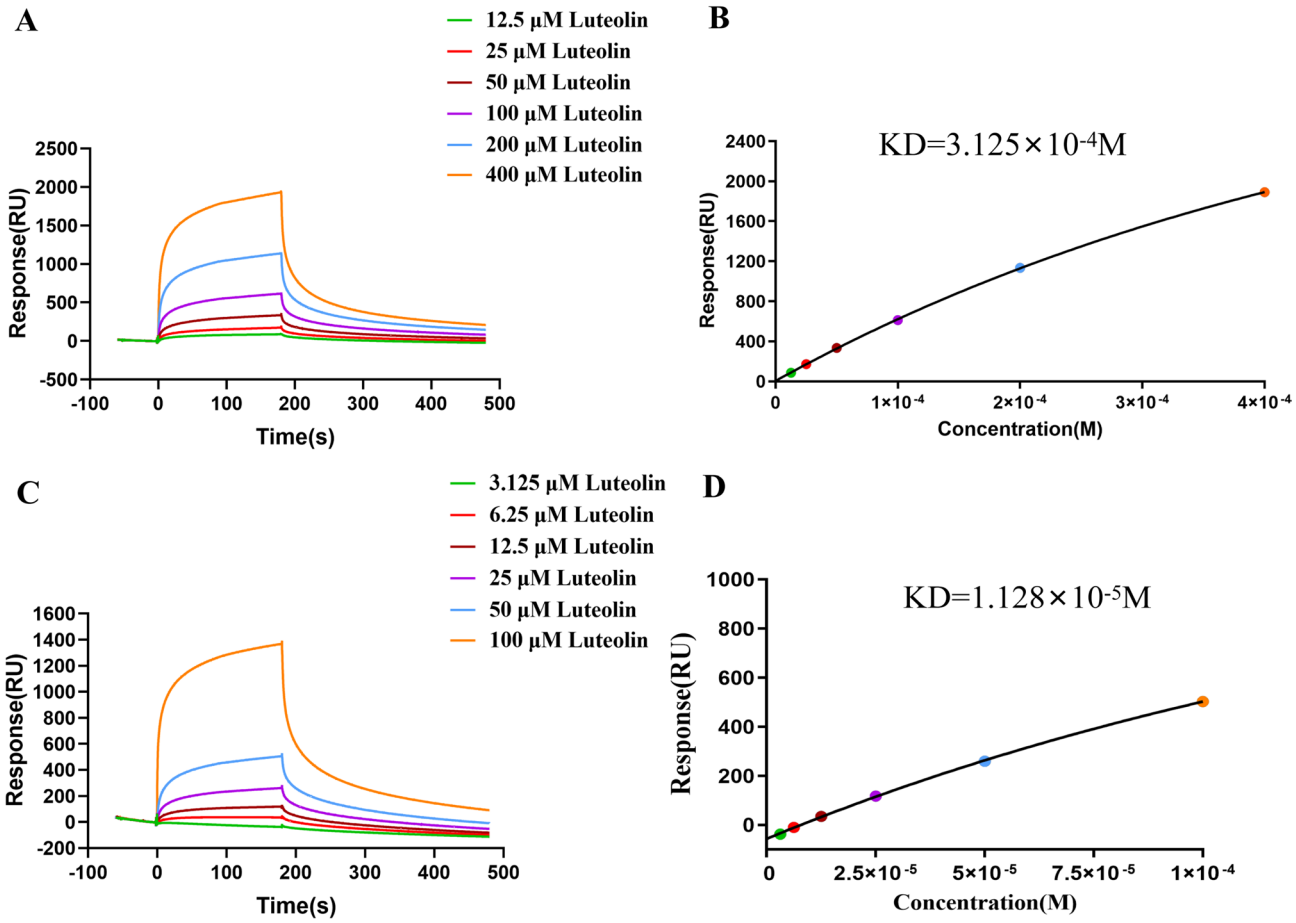

Fig. 5. Detection of the interaction between luteolin and the PknB and STP proteins by SPR. (**A**) Affinity sensing diagram for a series of concentrations of luteolin with PknB protein. (**B**) Affinity fitting curve of luteolin with the PknB protein. (**C**) Affinity sensing diagram for a series of concentrations of luteolin with STP protein. (**D**) Affinity fitting curve of luteolin with the STP protein.

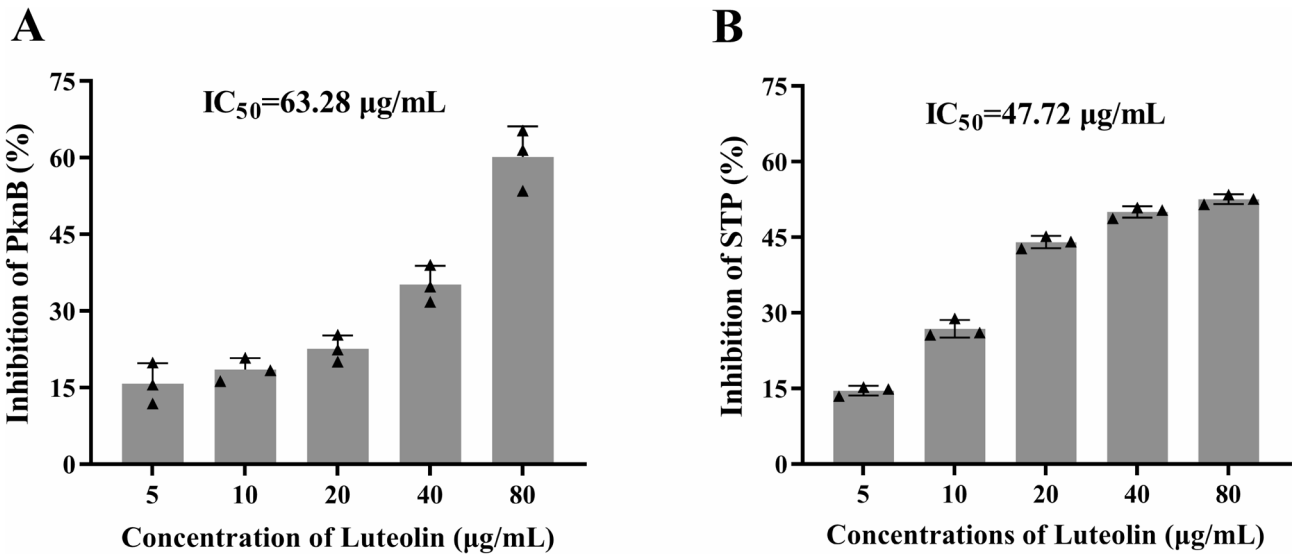

Fig. 6. The effects of luteolin on the activitiy of PknB and STP. (**A**) Inhibitory effect of luteolin at different concentrations on PknB activity. (**B**) Inhibitory effect of luteolin at different concentrations on STP activity.

Data availability

Data is provided within the manuscript or supplementary information files.

Received: 8 October 2024; Accepted: 23 June 2025
Published online: 03 July 2025

References

1. Rzewuska, M. et al. Pathogenicity and virulence of *Trueperella pyogenes*: A review. *Int J Mol Sci.* **20**, 2737 (2019).
2. Marchionatti, E., Kittl, S., Sendi, P. & Perreten, V. Whole genome-based antimicrobial resistance, virulence, and phylogenetic characteristics of *Trueperella pyogenes* clinical isolates from humans and animals. *Vet. Microbiol.* **294**, 110102 (2024).
3. Mileva, R. et al. Oxytetracycline pharmacokinetics after intramuscular administration in cows with clinical metritis associated with *Trueperella Pyogenes* infection. *Antibiotics-Basel* **9**, 392 (2020).
4. Marchionatti, E. & Perreten, V. Novel macrolide-lincosamide-streptogramin B resistance gene *erm* 56 in *Trueperella pyogenes*. *mSphere* **8**, e002392 (2023).
5. Zhang, D. et al. *Trueperella pyogenes* isolated from dairy cows with endometritis in Inner Mongolia, China: Tetracycline susceptibility and tetracycline-resistance gene distribution. *Microb. Pathog.* **105**, 51–56 (2017).
6. Galán-Relaño, Á. et al. Antimicrobial susceptibility and genetic characterization of *Trueperella pyogenes* isolates from pigs reared under intensive and extensive farming practices. *Vet. Microbiol.* **232**, 89–95 (2019).
7. Liang, C. et al. *Staphylococcus aureus* Transcriptome data and metabolic modelling investigate the interplay of Ser/Thr kinase PknB, its phosphatase Stp, the *glmR/yvcK* regulon and the *cdaA* operon for metabolic adaptation. *Microorganisms* **9**, 2148 (2021).
8. Liu, H. et al. Stk and Stp1 participate in *Streptococcus suis* serotype 2 pathogenesis by regulating capsule thickness and translocation of certain virulence factors. *Microb. Pathog.* **152**, 104607 (2021).
9. Zhu, Y., Dou, Q., Du, L. & Wang, Y. QseB/QseC: A two-component system globally regulating bacterial behaviors. *Trends Microbiol.* **31**, 749–762 (2023).
10. Li, L. et al. Roles of two-component regulatory systems in *Klebsiella pneumoniae*: Regulation of virulence, antibiotic resistance, and stress responses. *Microb. Res.* **272**, 127374 (2023).
11. Isaka, M. et al. *Streptococcus pyogenes* TrxSR two-component system regulates biofilm production in acidic environments. *Infect Immun.* **89**, e0036021 (2021).
12. Schaefers, M. M. Regulation of virulence by two-component systems in *Pathogenic Burkholderia*. *Infect Immun.* **88**, e00927-e1019 (2020).
13. Burastero, O. et al. Specificity and reactivity of *Mycobacterium tuberculosis* Serine/threonine kinases PknG and PknB. *J. Chem. Inf. Model* **62**, 1723–1733 (2022).
14. Tang, J. et al. A link between STK signalling and capsular polysaccharide synthesis in *Streptococcus suis*. *Nat. Commun.* **14**, 2480 (2023).
15. Zhang, C. et al. The eukaryote-like serine/threonine kinase STK regulates the growth and metabolism of zoonotic *Streptococcus suis*. *Front. Cell Infect. Microbiol.* **7**, 66 (2017).
16. Janczarek, M., Vinardell, J. M., Lipa, P. & Karaś, M. Hanks-type serine/threonine protein kinases and phosphatases in bacteria: Roles in signaling and adaptation to various environments. *Int. J. Mol. Sci.* **19**, 2872 (2018).
17. Nagarajan, S. N., Lenoir, C. & Grangeasse, C. Recent advances in bacterial signaling by serine/threonine protein kinases. *Trends Microbiol.* **30**, 553–566 (2022).
18. Zeng, J. et al. Protein kinases PknA and PknB independently and coordinately regulate essential *Mycobacterium tuberculosis* physiologies and antimicrobial susceptibility. *PLoS Pathog.* **16**, e1008452 (2020).
19. Shi, M. et al. Luteolin, a flavone ingredient: Anticancer mechanisms, combined medication strategy, pharmacokinetics, clinical trials, and pharmaceutical researches. *Phytother. Res.* **38**, 880–911 (2024).
20. Taheri, Y. et al. Paving luteolin therapeutic potentialities and agro-food-pharma applications: Emphasis on in vivo pharmacological effects and bioavailability traits. *Oxid. Med. Cell Longev.* **2021**, 1987588 (2021).
21. Guo, Y. et al. The antibacterial activity and mechanism of action of luteolin against *Trueperella pyogenes*. *Infect. Drug Resist.* **13**, 1697–1711 (2020).
22. Zhang, D. et al. Luteolin showed a resistance elimination effect on gentamicin by decreasing MATE mRNA expression in *Trueperella pyogenes*. *Microb. Drug Resist.* **25**, 619–626 (2019).
23. Guo, Y. et al. Luteolin increases susceptibility to macrolides by inhibiting MsrA efflux pump in *Trueperella pyogenes*. *Vet. Res.* **53**, 3 (2022).
24. Zhang, L. et al. Effects of luteolin on biofilm of *Trueperella pyogenes* and its therapeutic effect on rat endometritis. *Int. J. Mol. Sci.* **23**, 14451 (2022).
25. Baier, A. & Szyszka, R. Compounds from natural sources as protein kinase inhibitors. *Biomolecules* **10**, 1546 (2020).
26. Zhou, S. et al. Novel protein kinase C phosphorylated kinase inhibitor-matrine suppresses replication of hepatitis B virus via modulating the mitogen-activated protein kinase signal. *Bioengineered* **13**, 2851–2865 (2022).
27. Zhou, Y. et al. Structural basis for the inhibition of the autophosphorylation activity of HK853 by luteolin. *Molecules* **24**, 933 (2019).
28. Wu, K. J. et al. Small molecule Pin1 inhibitor blocking NF-κB signaling in prostate cancer cells. *Chem. Asian J.* **13**, 275–279 (2018).
29. Lu, J. J. et al. Quinones derived from plant secondary metabolites as anti-cancer agents. *Anticancer Agents Med. Chem.* **13**, 456–463 (2013).
30. Leung, K. H. et al. Discovery of a small-molecule inhibitor of STAT3 by ligand-based pharmacophore screening. *Methods* **71**, 38–43 (2015).
31. Lyon, G. J. et al. Rational design of a global inhibitor of the virulence response in *Staphylococcus aureus*, based in part on localization of the site of inhibition to the receptor-histidine kinase, AgrC. *Proc. Natl. Acad. Sci. U S A* **21**, 13330–13335 (2000).
32. Lolli, G. et al. Inhibition of protein kinase CK2 by flavonoids and tyrphostins. A structural insight. *Biochemistry* **51**, 6097–6107 (2012).
33. Rao, X., Huang, X., Zhou, Z. & Lin, X. An improvement of the 2ˆ (-delta delta CT) method for quantitative real-time polymerase chain reaction data analysis. *Biostat. Bioinforma Biomath.* **3**, 71–85 (2013).
34. Liu, Y. et al. CB-Dock2: Improved protein-ligand blind docking by integrating cavity detection, docking and homologous template fitting. *Nucleic Acids Res.* **50**, W159–W164 (2020).
35. Trott, O. & Olson, A. J. AutoDock Vina: Improving the speed and accuracy of docking with a new scoring function, efficient optimization, and multithreading. *J. Comput. Chem.* **31**, 455–461 (2013).
36. Adasme, M. F. et al. PLIP 2021: Expanding the scope of the protein-ligand interaction profiler to DNA and RNA. *Nucleic Acids Res.* **49**, W530–W534 (2021).
37. Gaudreault, F., Morency, L. P. & Najmanovich, R. J. NRGsuite: A PyMOL plugin to perform docking simulations in real time using FlexAID. *Bioinformatics* **31**, 3856–3858 (2015).
38. Das, S. et al. Surface plasmon resonance as a fascinating approach in target-based drug discovery and development. *Trends Anal. Chem.* **171**, 117501–117501 (2024).

39. King, A. & Blackledge, M. S. Evaluation of small molecule kinase inhibitors as novel antimicrobial and antibiofilm agents. *Chem. Biol. Drug Des.* **98**, 1038–1064 (2021).
40. Li, H. et al. Inhibitors targeting the autophosphorylation of serine/threonine kinase of *Streptococcus suis* show potent antimicrobial activity. *Front. Microbiol.* **13**, 990091 (2022).
41. Chen, D. et al. Sclerotiorin inhibits protein kinase G from *Mycobacterium tuberculosis* and impairs mycobacterial growth in macrophages. *Tuberculosis (Edinb).* **103**, 37–43 (2017).
42. Swain, S. P. et al. Flavanones: A potential natural inhibitor of the ATP binding site of PknG of *Mycobacterium tuberculosis*. *J. Biomol. Struct. Dyn.* **40**, 11885–11899 (2022).
43. Zheng, W. et al. Structure-based identification of a potent inhibitor targeting Stp1-mediated virulence regulation in *Staphylococcus aureus*. *Cell Chem. Biol.* **23**, 1002–1013 (2016).
44. Zhang, Z. et al. Molecular basis for luteolin as a natural TatD DNase inhibitor in *Trueperella pyogenes*. *Int. J. Mol. Sci.* **23**, 8374 (2022).
45. Diyah, N. W., Indriani, D. A., Dessidianti, R. & Siswandono, S. *In silico* analysis of luteolin derivatives as antibacterial agents targeting DNA gyrase and CTX-M-15 extended-spectrum β-lactamase of *Escherichia coli*. *J. Adv. Pharm. Technol. Res.* **15**, 29–36 (2024).
46. Fakhar, M., Ahmed, M. & Nasim Sabri, A. Computational and experimental strategies for combating MBL *P. aeruginosa* (MBLPA) biofilms using phytochemicals: Targeting the quorum sensing network. *Saudi J. Biol. Sci.* **31**, 104001 (2024).
47. Geng, Y. F. et al. An innovative role for luteolin as a natural quorum sensing inhibitor in *Pseudomonas aeruginosa*. *Life Sci.* **274**, 119325 (2021).
48. Fu, J. et al. Luteolin induces carcinoma cell apoptosis through binding Hsp90 to suppress constitutive activation of STAT3. *PLoS ONE* **7**, e49194 (2012).
49. Rivera, M. L. C. et al. Effect of capsicum frutescens extract, capsaicin, and luteolin on quorum sensing regulated phenotypes. *J. Food Sci.* **84**, 1477–1486 (2019).

Acknowledgements

We sincerely thank Tian Lan and Sheng Yang of Northeastern University for their assistance in the affinity assay.

Author contributions

M.C.L. and Y.R.G. conceived and designed this project and experiments. Y.T.G. and H.Y.S. performed the experiments. L.H.Y. participated for the preparation of animal experiments. Y.T.G., H.Y.S., Y.Y.W., C.L.T. and D.X.Z. participated in experiment design and data analysis. Y.T.G. wrote the original draft preparation. Y.R.G. and M.C.L. participated in revising the manuscript. All the authors have read and approved the final manuscript.

Funding

This study was supported by the National Nature Science Foundation of China, Grant Number 31972736.

Declarations

Competing interests

The authors declare no competing interests.

Additional information

Supplementary Information The online version contains supplementary material available at https://doi.org/10.1038/s41598-025-08698-5.

Correspondence and requests for materials should be addressed to Y.G. or M.L.